



Adsorption Isotherms and Isotheric Heat of Adsorption of Metal Organic Frameworks as Gas Storage for Liquefied Petroleum Gas Vehicle in Iraq

Mohammed Sattar Jabbar and Rana Th. Abd Alrubaye

Chemical Engineering Department, College of Engineering - University of Baghdad, Baghdad, Iraq.

Abstract

This research provides a novel technique for using metal organic frameworks (HKUST-1) as a gas storage system for liquefied petroleum gas (LPG) in Iraqi vehicles to avoid the drawbacks of the currently employed method of LPG gas storage. A low-cost adsorbent called HKUST-1 was prepared and characterized in this research to investigate its ability for propane storage at different temperatures (25, 30, 35, and 40 °C) and pressures of (1-7) bar. HKUST-1 was made using a hydrothermal method and characterized using powder X-ray diffraction, BET surface area, scanning electron microscopic (SEM), and Fourier Transforms infrared spectroscopy (FTIR). The HKUST-1 was produced using a hydrothermal technique and possesses a high crystallinity of up to 97%, surface area 3400 m²/g, and pore volume 0.7 cm³/g. The prepared adsorbent (HKUST-1) tested using volumetric method, the maximum adsorption capacity of propane was (10.499 mmol/g) at a temperature of 298K and a pressure of 7 bar. Furthermore, adsorption isotherm study was conducted to understand the system equilibrium (i.e., the fitting with one of the known models Langmuir, Freundlich, and Temkin isotherm models). It was observed that the Freundlich isotherm model fitted well the experimental data. The Clausius-Clapeyron equation was used to determine the heat of adsorption, and the results revealed that the heat of adsorption increased as the propane adsorption capacity increased. The prepared HKUST-1, which has a large surface area and a high adsorption capacity, can be used as a major solution for gas storage for liquefied petroleum gas (LPG) in Iraqi vehicles.

Keywords: metal organic frameworks, liquefied petroleum gas, adsorbed natural gas, Isotheric heat of Adsorption

Received on 21/03/2022, Accepted on 11/07/2022, published on 30/09/2022

<https://doi.org/10.31699/IJCPE.2022.3.4>

1- Introduction

Liquefied petroleum gas (LPG) (also called as "Propane Autogas") is mostly composed of propane (C₃H₈) with percentage (100% or 60% or 35%) and butane (C₄H₁₀) with percentage (40% or 65%) depending on the country and region, with some unsaturated components propene (C₃H₆) and butene (C₄H₈). LPG is produced by "wet" natural gas or refining petroleum (crude oil).

The LPG component are gases at ambient temperature and pressure, but is liquefied at high pressures (more than 20 bars) [1].

Currently, LPG is a preferred internal-combustion engine fuel because it emits less pollution and leaves little solid residue, does not dilute lubricants, and has a high octane rating, therefore, it is considered as a clean alternative for gasoline [2].

The Iraqi government is aiming to urge citizens to switch to clean, domestically produced fuel.

In Iraq, LPG (Propane Autogas) is being used as a clean vehicle fuel gas due to its low carbon emissions, low contamination risk, and environmentally friendly [3].

Although LPG burns cleaner than other fuel oils, it does have some drawbacks, such as higher fuel consumption due to its lower volumetric energy density than gasoline, and LPG pressure vessels are only filled to 80% of their overall capacity to allow for thermal expansion of the contained liquid, necessitating a larger storage tank [4].

Furthermore, because LPG has a low boiling point of about -50°C, it must be stored in pressurized steel tanks with a pressure of 20 bars or higher in order to convert the gases to their liquid state at room temperature [1].

The LPG drawbacks lead to the need of a heavier and larger metal tank with high-pressure. However, passenger car tanks should be light and constructed of carbon fibers, which are related to safety, cost, and space problems requirements, since the LPG tanks with these specifications are dangerous and expensive. As result, it was essential to find alternative method to store these gases for storing large amounts of gas.

Different techniques have been used to store natural gas, such as compressed natural gas (CNG) at 200-300 bar or liquefied natural gas (LNG) at -161.5 °C [5].

The principal disadvantage of CNG is the need for the large and heavy tanks, as well as expensive multi-stage compression [6]

Whereas, the disadvantages of LNG are the energy and cost associated with liquefaction at $-161.5\text{ }^{\circ}\text{C}$ [7]. Presently, a new gas storage technique (Adsorbed natural gas (ANG)) is being employed as an alternative technology for storing natural gas under suitable conditions for mobile usage. This new technology (ANG) stores the hydrocarbon gasses in porous materials placed in the tanks. Porous materials act like a sponge, catching gas molecules [8]. This method allows for the same amount of gas to be stored as CNG at a significantly lower pressure (40-50 bars), lowering operating expenses. Furthermore, increasing the driving distance of a natural gas vehicle (NGV) by employing adsorbed natural gas technology with higher pressure [9].

Many types of adsorbents, including zeolites, activated carbons [10], and Metal Organic Frameworks (MOFs) [5] [11] [12], were developed and evaluated for adsorbed natural gas (ANG). MOFs have been shown to have a higher methane storage capacity than other adsorbents [13] [14] [15].

MOFs are a new class of crystalline porous materials that have drawn a lot of attention in the last two decades due to their large surface area (up to $5000\text{ cm}^2/\text{g}$), pore volume (up to $2\text{ cm}^3/\text{g}$), high thermal and chemical stabilities, and low densities (from 0.21 to 1 g/cm^3) [16], as well as their potential uses in gas storage, molecular separation, and other applications [17]. MOFs have features over activated carbon and zeolite because of their simple tunable and adaptable structures, and high crystallinity [18]. Additionally, it allows for the optimization of pore dimension and surface chemistry within metal-organic frameworks, which was previously impossible in zeolite materials [17]. MOFs are the preeminent forum for producing unique multifunctional products when it comes to gas storage applications [19].

The current study employs an adsorption technique for LPG storage to solve the drawbacks of the LPG storage method presently used using a novel adsorbent. The adsorption technique involves filling tanks with porous storage materials to store LPG. Previous studies on propane adsorption on activated carbons [20], zeolites 5A [21], and MOFs were done in the separation field [22].

Abedini et al. (2020) showed that MOFs (HKUST-1) have a greater adsorption capacity for propane than activated carbon and zeolites 5A when utilized to separate the mixture of propylene/propane [23]. HKUST-1 has been utilized for propane separation until recently, but there has been no research for employing it as gas storage for propane.

The HKUST-1 (Hong Kong University of Science and Technology) is considered as one of the most important MOFs due to its high pore volume, good water adsorption/desorption stability, large surface area, and chemical stability [10].

Taking all of the facts into account, a new safe method of storing LPG gases that are used as fuel in vehicles is required to replace the greater cost and lower capacity of the current LPG vessel.

As a result, HKUST-1 was prepared, characterized, and investigated in this study in order to reduce the cost of current LPG vessels in vehicles. HKUST-1 has been selected for this task because of its high surface area and micro pore volume that enable for effective adsorption-desorption for storing and delivering high amounts of LPG.

2- Experimental Work

2.1. Materials

HKUST-1 was produced using copper (II) nitrate trihydrate [$\text{Cu}(\text{NO}_3)_2 \cdot 3\text{H}_2\text{O}$, 99 percent] and benzene 1, 3, 5 tricarboxylic acid (trimesic acid) (BTC 95 percent) from Sigma Aldrich. Absolute ethanol ($\text{C}_2\text{H}_5\text{OH}$) was from Fisher Scientific. The Propane autogas (adsorbed gas) was supplied from a Gulf gas company in Baghdad (89.97 Vol. %).

2.2. Preparation of HKUST-1

HKUST-1 was produced using the hydrothermal process reported by Hill et al. [24]. Trimesic acid (0.42 g) was accurately measured and dissolved in 24 ml of a 1:1 solvent ratio ($\text{C}_2\text{H}_5\text{OH}:\text{H}_2\text{O}$). Following that, the solution was mixed for ten minutes. After that, the copper nitrate trihydrate (0.875 g) was added to the solution and well stirred for 10 minutes.

The resulting blue solution was transferred to a 150 ml stainless steel Teflon lined autoclave and heated to 100°C for 30 hours in a furnace for crystallization once it was completely dissolved in the solvent.

The reactor was then cooled to room temperature, resulting in the formation of a green crystalline powder, as illustrated in Fig. 1. The powder was filtered and thoroughly washed in a 60 ml water-ethanol solution (1:1 Vol percent). Finally, the green powder was activated under vacuum at 100°C for 16 hours using a rotary dryer evaporator and stored in a closed vessel.



Fig. 1. Synthesized HKUST-1

2.3. Characterization of HKUST-1

After degassing the sample to remove moisture content and other gases that induce blockage and lower surface area, the Surface area analyzer (Micrometrics ASAP2020, USA) was applied to measure the surface area and pore volume by nitrogen physical adsorption at 77 K, According to ISO 9277-2010. A large surface area value indicates that the adsorbent's activity has increased as the activity site has increased [25].

An X-ray diffract meter (Shimadzu SRD 6000) with a 3-70° scan range, 40 kV tube voltage, 30 mA tube current, and 40 kV tube voltage was used to evaluate the samples. The structural and chemical bonds between MOF molecules were studied using an FTIR 8400S (600-4000) cm⁻¹ Shimadzu.

The HKUST-1 morphology was described using scanning electron microscopic analysis.

2.4. Propane Isotherms Adsorption

An experimental setup based on the volumetric method was used to estimate the equilibrium adsorption capacity of synthesized adsorbents, as shown in Fig.2. The fittings are all connected to the copper pipes (1/4 inch). Stainless steel cylinders measuring around 25 cm³ used as reservoirs and adsorption cells.

The gas pressure was recorded with a gauge (Helicoid gauge) that ranged from (1-10 bar) and had a sensitivity of 0.02 percent and an accuracy of 1%. Both the reservoir and the adsorption chamber are maintained at the same temperature using a water bath.

Before each experiment, a vacuum pump was used to evacuate the adsorption equilibrium measurement equipment. A cylinder connected to a pressure regulator supplies the feeding gas. The gas exit flow rate is controlled by a rotameter. Temperatures of (25, 30, 35, 40) °C and pressures of (1, 3, 5, 7) bar would be used to estimate propane isotherms. Nitrogen gas was used to determine the volume of the overall unit.

The initial outgassing process was performed overnight under vacuum at 100°C. The degassed sample was then inserted in the adsorption chamber in a quantity of 0.2 g.

All the valves were closed at the end of the degassing process to prepare the system for the experiments run. In experiment run, V3 and V4 valves opened, the gas was pumped into the reservoir chamber until it reached to equilibrium. V3 was closed when the pressure reached the equilibrium; V4 was remained open, and the pressure value was recorded.

The V5 was then opened, allowing the gas to enter the adsorption chamber and achieving equilibrium. The amount of adsorbed gas was determined at equilibrium using the equations below [26]:

$$q = \frac{(C_i - C_f)V_r - C_f \epsilon V_a}{W} \quad (1)$$

Where: (q) is amount of gas adsorbed (mmol/g), (C) is concentration (mmol/L), (V) is volume of the vessel (L), (ε) void fraction, (W) weight of adsorbent (g), subscripts i,f,r,a refer to initial, final, reservoir and adsorber respectively.

C_i and C_f where calculate from equation of real gases [27]:

$$P V = Z n R T \quad (2)$$

Where: $C = n/V$

$$C_i = \frac{P_i}{Z_i R T} \quad (3)$$

$$C_f = \frac{P_f}{Z_f R T} \quad (4)$$

Z compressibility factor of feed and out gases may be estimated according to the generalized equation [27]:

$$Z = 1 + \frac{B P}{R T} \quad (5)$$

The coefficient of B can be determined as follows [27]:

$$B = \frac{R T C}{P C} (B^0 + \omega B') \quad (6)$$

The coefficient of B⁰ and B' may be calculated as follows [27]:

$$B^0 = 0.083 - \frac{0.422}{T_r^{1.6}} \quad (7)$$

$$B' = 0.139 - \frac{0.172}{T_r^{4.2}} \quad (8)$$

Where: P_c is critical pressure of propane (42.48 bar), T_c is critical temperature of propane (369.8 K), R gas constant (8.314 L.Kpa/ mol. K) and ω is centric factor (0.152).

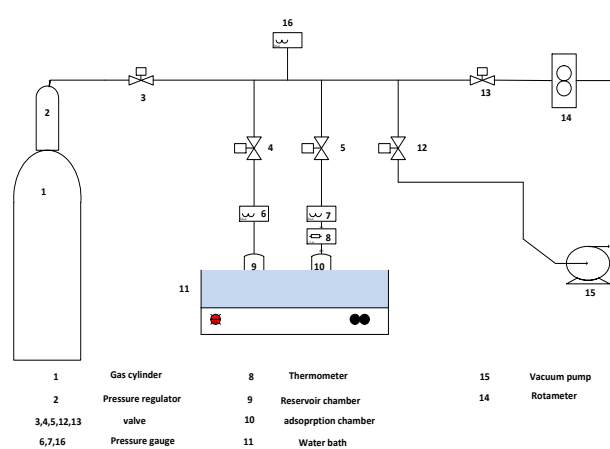


Fig. 2. Schematic diagram of apparatus used for adsorption equilibrium measurement

2.5. Adsorption Isotherms

The adsorption behavior of gas (or vapor) is investigated by varying the applied gas (or vapor) pressure; the relationship between the amount of adsorbed and pressure is referred to as an adsorption isotherm ("iso" and "therm" denote equal and temperature, respectively) [28].

The adsorption isotherms were studied using the Langmuir, Freundlich, and Temkin isotherms, Eqs. (9, 10, and 11) respectively.

Langmuir equation is [29]:

$$\frac{1}{q_e} = \left(\frac{1}{q_m K_L}\right) \frac{1}{C_e} + \frac{1}{q_m} \quad (9)$$

Freundlich equation is [30]:

$$\text{Log}(q_e) = \text{Log}(K_f) + \frac{1}{n} \text{Log}(C_e) \quad (10)$$

Temkin equation is [31]:

$$q_e = \beta \ln A + \beta \ln C_e \quad (11)$$

Where: q_e [mmol g⁻¹] is the amount of gas uptake on adsorbent at equilibrium, C_e [mmol L⁻¹] is the equilibrium concentration of gas, q_m [mmol g⁻¹] is the adsorption capacity constant (the equilibrium adsorption amount for a full monolayer), K_f is Freundlich adsorption equilibrium constant, K_L [L mmol⁻¹] is Langmuir adsorption equilibrium constant, β related to the heat of adsorption and $A(K_f)$ is equilibrium binding constant [J mmol⁻¹].

2.6. Isotheric Heat of Adsorption

The isotheric heat of adsorption (Q_{st}) (isotheric indicating constant loading) is also known as the heat of adsorption or enthalpy of adsorption. When developing adsorption processes, the isotheric heat of adsorption, which measures the change in adsorbent temperature during adsorption, is an important thermodynamic property to consider. Adsorption heat is proportional to the binding energy between adsorbed molecules and the adsorbent, as well as interactions between adsorbates [32].

The two techniques of determining Q_{st} are experiment-based calculations and molecular simulations. The latter's simulated adsorption enthalpies are largely dependent on isotherms derived from grand canonical Monte Carlo simulations (GCMS) utilizing the ensemble fluctuation approach [33].

Direct and indirect calculations are two types of experiment-based calculations. In the direct technique, which employs a calorimetric-volumetric system, it is feasible to measure directly the emitted heat during adsorption using a calorimeter. Because these systems are extremely complex and expensive, only a few studies use the direct approach to calculate Q_{st} [34].

The indirect method of calculating the isotheric enthalpy of adsorption as a function of the amount adsorbed (loading) using adsorption isotherms is by far the most general. In most cases, the adsorbate-adsorbent interaction energy is computed indirectly utilizing at least two adsorption isotherms (T_1, T_2) measured at close but different temperatures ($\Delta T \approx 10\text{-}20$ K). The most common method for obtaining adsorption isotherms is volumetric gas adsorption measurements [35]. The isotheric heat of adsorption (Q_{st}) can be estimated by the Clausius-Clapeyron equation as [22]:

$$Q_{st} = -RT^2 \left(\frac{\partial \ln p}{\partial T} \right) q \quad (12)$$

The integration leads to:

$$\ln p = \frac{Q_{st}}{RT} + C \quad (13)$$

Where: Q_{st} (kJ/mol) is isotheric heat of adsorption, T is temperature (K), P is the pressure (KPa), R is the gas constant and q is the adsorption amount (mmol/g).

3- Result and Discussion

3.1. Characterization of HKUST-1

The XRD analysis showed a typical characterization peaks of HKUST-1 with high purity phase, and a crystallinity of 97%, which is close to Al-Yassiry's work, which had 100% crystallinity under the similar conditions [36]. The HKUST-1 BET analysis has a pore volume of (0.7 cm³/g) and a surface area of 3480 m²/g, which was similar to Kareem's results (3635 m²/g) under the same operating conditions [18].

All of the IR analysis bands for HKUST-1 were in good agreement with the IR analysis [37]. The presence of the -COOH groups in the organic ligand reacting with metal ions is indicated by a strong stretching vibration of carboxylate anions at (1608.63)1/cm as seen in Fig. 3. A band painted at (3600-2800) 1/cm demonstrated the presence of water and -OH groups in the material's structure. The absence of CuO and Cu₂O in the synthesis product during the production of HKUST-1 is indicated by peaks at (410, 500, 610, and 615) 1/cm. Increased and changed carboxyl absorption from (3,100) to (3,600) 1/cm in HKUST-1 revealed the loss of water molecules [38].

Fig. 4 demonstrates that the IR analysis for HKUST-1 does not change after the propane adsorption process, indicating that the adsorbent's composition did not change after desorption.

SEM images of the prepared HKUST-1 at a magnification of 2062 x are shown in Fig. 5. As seen in this figure, the synthesized metal-organic framework has an octahedral shape. This result is similar to the one found by Lin, et al. [39].

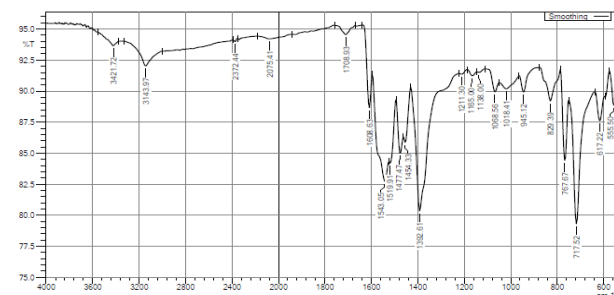


Fig. 3. FTIR of prepared HKUST-1 before adsorption

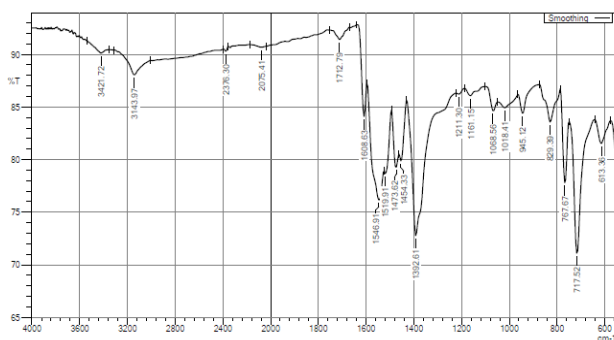


Fig. 4. FTIR of prepared HKUST-1 after adsorption

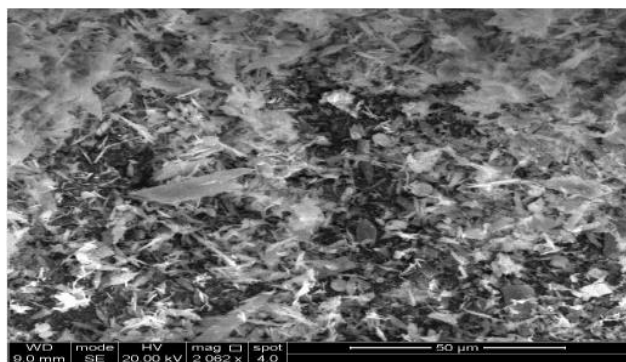


Fig. 5. SEM image of the synthesized HKUST-1

3.2 Propane Adsorption on HKUST-1

a. Temperature Effect on Propane Adsorption Capacity

The relationship between the propane adsorption capacity q (mmol/g) and temperature is seen in Fig. 6. At a pressure of 7 bar and a temperature of 298 K, the highest adsorption capacity was found to be 10.49 mmol/g.

As can be seen in Fig. 6, increasing the temperature causes the amount of adsorbed propane on the adsorbent to decrease, particularly at 7 bars. Fig. 6 illustrates that increasing the temperature at constant pressure decreases the total quantity of adsorbed propane on the adsorbent, indicating that the process is exothermic.

This can be explained by the fact that when the temperature increased, the propane adsorbed on the HKUST-1 surface became unstable, leading in desorption of more propane molecules. Lamia, et al. [40] found

similar behavior of decreasing adsorption capacity when temperature is increased.

Additionally, the adsorption capacities in this study (7.44 mmol/g at 1 bar and 303K) were close to those predicted by Rubes, et al [41] (at similar condition employing HKUST-1 as an adsorbent for adsorption of propane and propylene), which were (7.3) mmol/g.

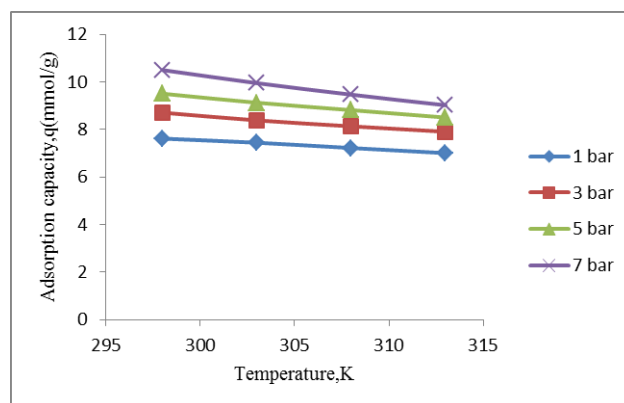


Fig. 6. Adsorption capacity as a function of temperature

b. Pressure Effect on Propane Adsorption Capacity

The influence of pressure on propane adsorption capacity was studied at a constant temperature in the range of 1 to 7 bars (25, 30, 35 and 40 °C). When pressure is increased, the propane adsorption capacity increases, as seen in Fig. 7. This is because increased pressure increases momentum, which reduces the resistance to mass transfer between the adsorbent and the adsorbate, resulting in a greater number of gas molecules on the adsorption site.

This figure also shows a relatively high adsorption capacity at 1 bar (7.61 mmol/g) due to the significant interaction between large numbers of carbon atoms in the structure of propane and the HKUST- 1 surface. Ponraj et al. [42] used a simulated isotherm of HKUST-1 as an adsorbent to separate methane from ethane and propane at 298 K with pressures ranging from 0.001 to 100 bar, and found the similar behavior of greater adsorption capacity at low pressure.

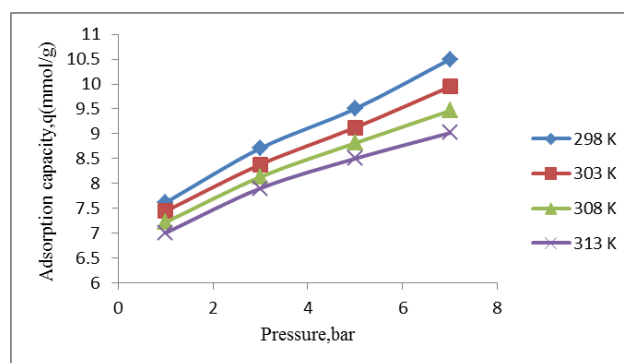


Fig. 7. Adsorption capacity as a function of pressure

3.3. Adsorption Isotherms

The Langmuir, Freundlich, and Temkin isotherms were used to investigate the adsorption isotherms. These isotherms link propane intake per unit mass of adsorbent (q_e) to the concentration of adsorbate in the gas phase at equilibrium (C_e).

a. Langmuir Isotherm

Equilibrium data for propane adsorption on the HKUST-1 were fitted using the linearized Langmuir equation described in eq. 9. Fig. 8 shows a linear plot of equilibrium concentration ($1/C_e$) versus equilibrium adsorption ($1/q_e$). The Langmuir constants (K_L and q_m) were calculated using the slope ($1/q_m K_L$) and the intercept of the plot ($1/q_m$), as shown in Table 1. The observed correlation coefficients (R^2) at 298, 303, 308, and 313 K were 0.8063, 0.8047, 0.8278, and 0.8392, respectively, according to the results obtained and listed in Table 1; the isotherm data does not fit the Langmuir equation.

b. Temkin Isotherm

Equilibrium data for propane adsorption on the HKUST-1 were fitted using the linearized Temkin equation described in eq. 11. Fig. 9 shows a linear plot of equilibrium concentration ($\ln C_e$) vs. adsorption capacity (q_e). The Temkin constants (K_T and β) were calculated using the slope (β) and intercept of the plot ($\beta \ln K_T$), as shown in Table 1.

The observed correlation coefficients (R^2) at 298, 303, 308, and 313 K were 0.9076, 0.9135, 0.9346, and 0.9465, respectively, according to the results obtained and listed in Table 1; the isotherm values fit the Temkin equation well.

c. Freundlich Isotherm

The propane adsorption equilibrium data were carefully investigated using the Freundlich isotherm. To fit the equilibrium data for propane adsorption on the HKUST-1, the linearized Freundlich equation described by eq. 10 was employed. Fig. 10 shows a linear plot of ($\log C_e$) vs ($\log q_e$). The Freundlich constants (K_f and n) were calculated using the slope ($1/n$) and the plot intercept ($\log K_f$) and listed in Table 1. The observed correlation coefficients at 298, 303, 308, and 313 K were 0.9345, 0.9369, 0.9531, and 0.9613, respectively, according to the results obtained and listed in Table 1; the isotherm values fit the Freundlich equation well. The results show that adsorption experimental data is suitable for Temkin and Freundlich models; however, when the R^2 values for the Freundlich and Temkin models are compared, the R^2 values for the Freundlich model are greater than those for the Temkin model.

These results indicate that the Freundlich model is more suitable with propane adsorption on HKUST-1.

In this research, the values of n at equilibrium were more than unity, indicating that the slope ($1/n$) was closer to zero, indicating a more heterogeneous adsorption process.

Table 1. Isotherm parameters for propane adsorption on HKUST-1

Isotherm Parameters	Temperature (298 K)	Temperature (303 K)	Temperature (308 K)	Temperature (313 K)
Langmuir (q_m)	9.8232	9.3809	9.0171	8.6655
Langmuir (K_L)	0.3467	0.3826	0.4053	0.4561
Langmuir (R^2)	0.8063	0.8047	0.8278	0.8392
Freundlich (K_f)	5.9375	5.9020	5.8237	5.8398
Freundlich (n)	9.7561	10.5708	11.1982	12.3762
Freundlich (R^2)	0.9345	0.9369	0.9531	0.9613
Temkin (β)	0.9056	0.8041	0.7316	0.6404
Temkin (K_T)	383.1521	878.5400	1699.2534	5708.72027
Temkin (R^2)	0.9076	0.9135	0.9346	0.9465

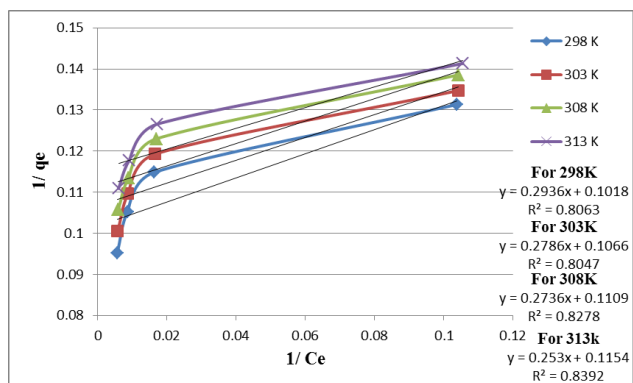


Fig. 8. Langmuir isotherm

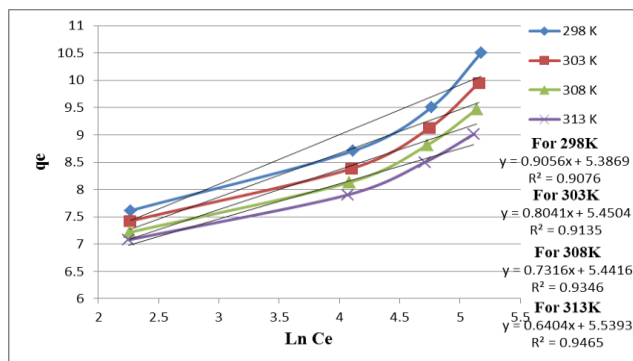


Fig. 9. Temkin isotherm

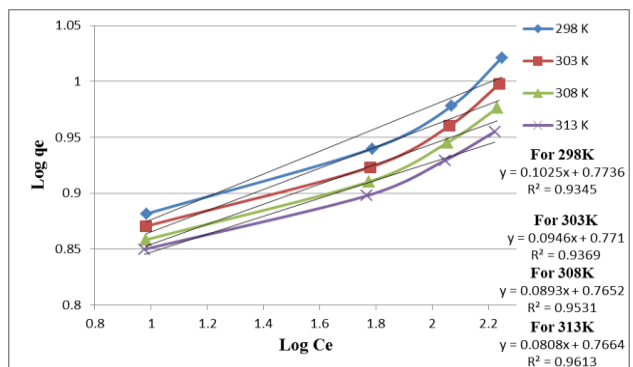


Fig. 10. Freundlich isotherm

3.4. Isotheric Heat of Adsorption

For the Clausius-Clapeyron technique, the two adsorption isotherms must be fitted with the same continuous function, such as a Langmuir, dual-site Langmuir, Toth, Sips, Jovanovic, Dubinin-Radushkevich, Freundlich-Langmuir, or other fit [43].

a. Clausius-Clapeyron Approach for Isotheric Heat of Adsorption Calculation

The same model must be used for the two isotherms at two temperatures (298 and 313 K). Most MOFs have a Freundlich-Langmuir isotherm, which can be fitted using the equation below [35].

$$q = \frac{a * b * (P)^c}{1 + b * (P)^c} \quad (14)$$

Where: q is the amount adsorbed (the loading) in mmol g^{-1} , a is the maximal loading in mmol g^{-1} , P the pressure in kPa, c the heterogeneity exponent and b the affinity constant ($1/\text{kPa}^c$).

By using Origin program the curve in Fig.7 is fitting to Fig. 11.

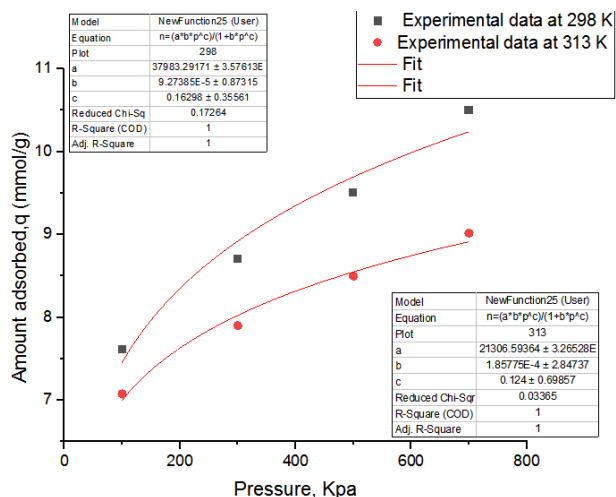


Fig. 11. Adsorption isotherms after fitting by Freundlich-Langmuir isotherm using Origin Program

Rearrange equation (14) and substitute the fitting parameters (a, b , and c) to determine the pressure at any temperature and the same loading.

Equation (14) become:

$$P(q) = \sqrt[c]{\frac{q}{a * b - q * b}} \quad (15)$$

Now, plot $\ln(P)$ versus T at the same loading as shown in Fig. 12 and find slope of every line which result and calculate Q_{st} ($Q_{st} = \text{slope} * R$) where R is universal gas constant and plot Q_{st} versus amount adsorbed(q) as shown in Fig. 13.

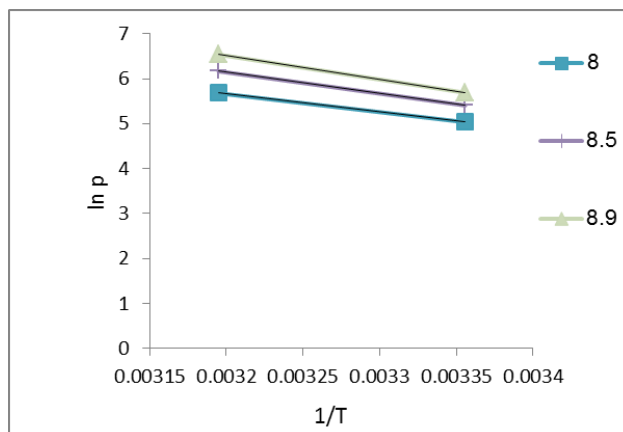


Fig. 12. $\ln P$ v.s $1/T$

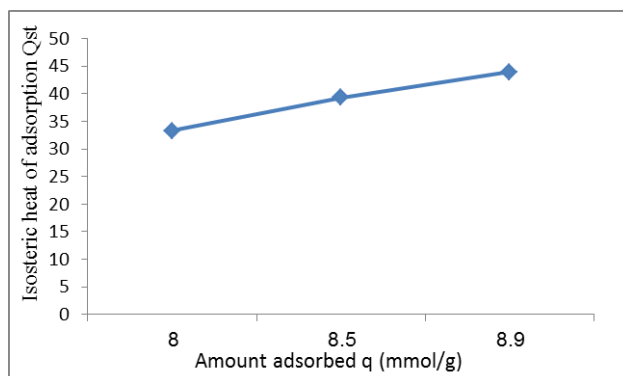


Fig. 13. Isotheric heat of adsorption as a function of the amount adsorbed

The isotheric heat of adsorption increased as the adsorption capacity increased, as seen in Fig. 13. Significant lateral interactions between adsorbates at HKUST-1 sites cause this increase. The propane molecules preferentially bind at cage center sites, followed by adsorption at cage window sites, as explained by Rubes [36]. The adsorption enthalpies rise as propane loading increases because the adsorbates at the cage center and cage window sites have strong lateral interactions.

When the isotheric heat of adsorption increased with coverage (due to increasing the lateral interaction between adsorbate-adsorbate interactions while decreasing the binding energy between adsorbate molecules and the adsorbent surface), this resulted in a decrease in the amount of propane molecules that could be adsorbed and a decrease in the amount of gas delivered at desorption due to more gas molecules remaining in adsorbent sites due to the increased lateral interaction.

4- Conclusions

In this work, The HKUST-1 was successfully prepared and used as an effective adsorbent for propane gas. The HKUST-1 was produced using a hydrothermal technique and possesses a high crystallinity of up to 97%, surface area $3400 \text{ m}^2/\text{g}$, and pore volume $0.7 \text{ cm}^3/\text{g}$. Adsorption was utilized to store propane using the prepared HKUST-1.

According to the experiments, the largest propane adsorption capacity on HKUST-1 was obtained around (10.499 mmol/g) at temperature 25 °C and pressure 7 bar. According to the adsorption isotherm results, the equilibrium data were best described by the Freundlich isotherm model, which means heterogeneous surfaces of HKUST-1 (i.e., each site is occupied by multiple particles) and physical adsorption. The isosteric heat of adsorption increased as adsorption capacity increased. Significant lateral interactions between the molecules adsorbed on HKUST-1 sites caused this increase.

References

- [1] Müller, U., Hesse, M., Pütter, H. and Yaghi, O.M., BASF SE and University of Michigan, 2008. Metal-organic framework materials for gaseous hydrocarbon storage. U.S. Patent 7,343,747.
- [2] Demirbas, A., 2002. Fuel properties of hydrogen, liquefied petroleum gas (LPG), and compressed natural gas (CNG) for transportation. *Energy Sources*, 24(7), pp.601-610.
- [3] Arapatsakos, Karkanis, Katirtzoglou and Pantokratoras, 2008. Liquid Petroleum Gas (LPG) and Natural Gas (NG) as fuels on diesel engine-dual fuel engine. *Recent Advances in Fluid Mechanics and Heat & Mass Transfer*, 154-161.
- [4] Raslavičius, L., Keršys, A., Mockus, S., Keršienė, N. and Starevičius, M., 2014. Liquefied petroleum gas (LPG) as a medium-term option in the transition to sustainable fuels and transport. *Renewable and Sustainable Energy Reviews*, 32, pp.513-525.
- [5] Makal, T.A., Li, J.R., Lu, W. and Zhou, H.C., 2012. Methane storage in advanced porous materials. *Chemical Society Reviews*, 41(23), pp.7761-7779.
- [6] Mason, J.A., Veenstra, M. and Long, J.R., 2014. Evaluating metal-organic frameworks for natural gas storage. *Chemical Science*, 5(1), pp.32-51.
- [7] Dobrota, Đ., Lalić, B. and Komar, I., 2013. Problem of boil-off in LNG supply chain. *Transactions on maritime science*, 2(02), pp.91-100.
- [8] Chang, K.J. and Talu, O., 1996. Behavior and performance of adsorptive natural gas storage cylinders during discharge. *Applied Thermal Engineering*, 16(5), pp.359-374.
- [9] Mota, J.B., Rodrigues, A.E., Saadjan, E. and Tondeur, D., 1997. Dynamics of natural gas adsorption storage systems employing activated carbon. *Carbon*, 35(9), pp.1259-1270.
- [10] Chui, S.S.Y., Lo, S.M.F., Charmant, J.P., Orpen, A.G. and Williams, I.D., 1999. A chemically functionalizable nanoporous material [Cu₃ (TMA)₂ (H₂O)₃]_n. *Science*, 283(5405), pp.1148-1150.
- [11] Menon, V.C. and Komarneni, S., 1998. Porous adsorbents for vehicular natural gas storage: a review. *Journal of Porous Materials*, 5(1), pp.43-58.
- [12] Morris, R.E. and Wheatley, P.S., 2008. Gas storage in nanoporous materials. *Angewandte Chemie International Edition*, 47(27), pp.4966-4981.
- [13] Furukawa, H., Ko, N., Go, Y.B., Aratani, N., Choi, S.B., Choi, E., Yazaydin, A.Ö., Snurr, R.O., O’Keeffe, M., Kim, J. and Yaghi, O.M., 2010. Ultrahigh porosity in metal-organic frameworks. *Science*, 329(5990), pp.424-428.
- [14] Perry Iv, J.J., Perman, J.A. and Zaworotko, M.J., 2009. Design and synthesis of metal-organic frameworks using metal-organic polyhedra as supermolecular building blocks. *Chemical Society Reviews*, 38(5), pp.1400-1417.
- [15] Yaghi, O.M., O’Keeffe, M., Ockwig, N.W., Chae, H.K., Eddaoudi, M. and Kim, J., 2003. Reticular synthesis and the design of new materials. *Nature*, 423(6941), pp.705-714.
- [16] Eddaoudi, M., Moler, D.B., Li, H., Chen, B., Reineke, T.M., O’keeffe, M. and Yaghi, O.M., 2001. Modular chemistry: secondary building units as a basis for the design of highly porous and robust metal-organic carboxylate frameworks. *Accounts of chemical research*, 34(4), pp.319-330.
- [17] Li, J.R., Kuppler, R.J. and Zhou, H.C., 2009. “Selective gas adsorption and separation in metal-organic frameworks”, *Chemical Society Reviews*, 38(5), pp.1477-1504.
- [18] Kareem, H.M. and Alrubaye, R.T.A., 2019. “Synthesis and Characterization of Metal Organic Frameworks for Gas Storage”, In *IOP Conference Series: Materials Science and Engineering*, 518(6), p. 062013.
- [19] Li, H., Li, L., Lin, R.B., Zhou, W., Zhang, Z., Xiang, S. and Chen, B., 2019, “Porous metal-organic frameworks for gas storage and separation: Status and challenges”, *EnergyChem*, 1(1), p.100006.
- [20] Jarvelin, H. and Fair, J.R., 1993, “Adsorptive separation of propylene-propane mixtures”, *Industrial & engineering chemistry research*, 32(10), pp.2201-2207.
- [21] Divekar, S., Nanoti, A., Dasgupta, S., Chauhan, R., Gupta, P., Garg, M.O., Singh, S.P. and Mishra, I.M., 2016, “Adsorption equilibria of propylene and propane on zeolites and prediction of their binary adsorption with the ideal adsorbed solution theory”, *Journal of chemical & engineering data*, 61(7), pp.2629-2637.
- [22] Bao, Z., Alnemrat, S., Yu, L., Vasiliev, I., Ren, Q., Lu, X. and Deng, S., 2011, “Adsorption of ethane, ethylene, propane, and propylene on a magnesium-based metal-organic framework”, *Langmuir*, 27(22), pp.13554-13562.
- [23] Abedini, H., Shariati, A. and Khosravi-Nikou, M.R., 2020. Adsorption of propane and propylene on M-MOF-74 (M= Cu, Co): Equilibrium and kinetic study. *Chemical Engineering Research and Design*, 153, pp.96-106.

- [24] [Hill, P., Al-Janabi, N., Torrente-Murciano, L., Garforth, A., Gorgojo, P., Siperstein, F., & Fan, X., 2015. "Mapping the Cu-BTC metal-organic framework \(HKUST-1\) stability envelope in the presence of water vapour for CO₂ adsorption from flue gases", Chemical Engineering Journal, 281, pp. 669–677.](#)
- [25] [Li, Y., Wang, L.-J., Fan, H.-L., Shangguan, J., Wang, H., & Mi, J., 2015. "Removal of sulfur compounds by a copper-based metal organic framework under ambient conditions", Energy and Fuels, 29\(1\), pp. 298–304.](#)
- [26] Ahmed J .M, 2005, "Adsorption of Light Hydrocarbons by Molecular Sieves", Ph.D. Thesis, College of Engineering, Baghdad University.
- [27] Smith, J. M., Van Ness, H.C. and Abbot, M. M. (2005) Introduction to Chemical Engineering Thermodynamics, 7th ed., New York, McGraw-Hill.
- [28] [Furukawa, H. \(2018\) Synthesis and Characterization of Metal-Organic Frameworks.in: Glover, T.G. and Mu, B. \(eds.\) Gas adsorption in metal-organic frameworks: Fundamentals and applications. CRC Press., pp.19-70.](#)
- [29] [Langmuir, I., 1918. The adsorption of gases on plane surfaces of glass, mica and platinum. Journal of the American Chemical society, 40\(9\), pp.1361-1403.](#)
- [30] Freundlich, H.K., 1909. eine Darstellung der Chemie der Kolloide und verwandte Gebiete. Kapillarchemie. Leipzig.
- [31] Tempkin, M.I. and Pyzhev, V.J.A.P.C., 1940. Kinetics of ammonia synthesis on promoted iron catalyst. Acta Phys. Chim. USSR, 12(1), p.327.
- [32] [Tsvizdze, A.Y., Aksyutin, O.E., Ishkov, A.G., Knyazeva, M.K., Solovtsova, O.V., Men'shchikov, I.E., Fomkin, A.A., Shkolin, A.V., Khozina, E.V. and Grachev, V.A., 2019. Metal-organic framework structures: Adsorbents for natural gas storage. Russian Chemical Reviews, 88\(9\), p.925.](#)
- [33] [Du, Z., Nie, X., Deng, S., Zhao, L., Li, S., Zhang, Y. and Zhao, J., 2020. "Comparative analysis of calculation method of adsorption isosteric heat: Case study of CO₂ capture using MOFs", Microporous and Mesoporous Materials, 298, p.110053.](#)
- [34] [Sumida, K., Rogow, D.L., Mason, J.A., McDonald, T.M., Bloch, E.D., Herm, Z.R., Bae, T.H. and Long, J.R., 2012. Carbon dioxide capture in metal-organic frameworks. Chemical reviews, 112\(2\), pp.724-781.](#)
- [35] [Nuhnen, A. and Janiak, C., 2020. "A practical guide to calculate the isosteric heat/enthalpy of adsorption via adsorption isotherms in metal-organic frameworks, MOFs", Dalton Transactions, 49\(30\), pp.10295-10307.](#)
- [36] [Alyassiry, A.A. and Alrubaye, R.T.A., 2020, March. Desulfurization of model gasoline using metal organic frame-work. In AIP Conference Proceedings \(Vol. 2213, No. 1, p. 020090\). AIP Publishing LLC.](#)
- [37] [Hoang, T. C., Nguyen Thi, T. V., Luu, C. L., Nguyen, T., Bui, T. H., Duy Nguyen, P. H., & Pham Thi, T. P., 2013. "Synthesis of MOF-199 and application to CO₂ adsorption", Advances in Natural Sciences: Nanoscience and Nanotechnology, 4\(3\), p. 035016.](#)
- [38] [Alrubaye, R.T.A. and Kareem, H.M., 2019. "Carbon Dioxide Adsorption on MOF-199 Metal-Organic Framework at High Pressure", In IOP Conference Series: Materials Science and Engineering, 557\(1\), p. 012060.](#)
- [39] [Lin, K. S., Adhikari, A. K., Ku, C. N., Chiang, C. L., & Kuo, H. \(2012\) 'Synthesis and characterization of porous HKUST-1 metal organic frameworks for hydrogen storage', International Journal of Hydrogen Energy. Elsevier Ltd, 37\(18\), pp. 13865–13871.](#)
- [40] [Lamia, N., Jorge, M., Granato, M.A., Paz, F.A.A., Chevreau, H. and Rodrigues, A.E., 2009. "Adsorption of propane, propylene and isobutane on a metal-organic framework: Molecular simulation and experiment", Chemical Engineering Science, 64\(14\), pp.3246-3259.](#)
- [41] [Rubes, M., Wiersum, A.D., Llewellyn, P.L., Grajciar, L., Bludsky, O. and Nachtigall, P., 2013. Adsorption of propane and propylene on CuBTC metal-organic framework: combined theoretical and experimental investigation. The Journal of Physical Chemistry C, 117\(21\), pp.11159-11167.](#)
- [42] [Ponraj, Y.K. and Borah, B., 2020. Separation of methane from ethane and propane by selective adsorption and diffusion in MOF Cu-BTC: A molecular simulation study. Journal of Molecular Graphics and Modelling, 97, p.107574.](#)
- [43] [Tóth, J., 1995. Uniform interpretation of gas/solid adsorption. Advances in Colloid and Interface Science, 55, pp.1-239.](#)

الامتزاز الأيزوثيرمي وحرارة الامتزاز للأطر العضوية المعدنية المستخدمة لتخزين الغاز البترولي المسال في المركبات العراقية

محمد ستار جبار و رنا ثابت عبد الربيعي

جامعة بغداد, كلية الهندسة, قسم الهندسة الكيميائية

الخلاصة

يقدم هذا البحث تقنية جديدة لاستخدام الأطر العضوية المعدنية (HKUST-1) كنظام تخزين للغاز البترولي المسال (LPG) في المركبات العراقية لتجنب عيوب الطريقة المستخدمة حاليًا لتخزين غاز البترولي المسال. تم تحضير مادة مازة منخفضة التكلفة تسمى HKUST-1 وتم فحصها في هذا البحث للتحقق من قدرتها على تخزين البروبان في درجات حرارة مختلفة °C (25 ، 30 ، 35 ، 40) وضغوط (1-7) bar. تم تصنيع HKUST-1 باستخدام طريقة حرارية مائية وتم وصف خصائصه باستخدام حيود الأشعة السينية ، ومساحة سطح BET ، والمسح المجهر الإلكتروني (SEM) ، و الأشعة تحت الحمراء (FTIR). أظهرت نتائج الأشعة السينية لـ HKUST-1 المحضر نسبة تبلور جيدة 97%، بينما أظهرت نتائج تحليل المساحة السطحية الحصول على مساحة السطحية مقدارها (3480m²/g) وحجم مسامي (0.7cm³/g). تم اختبار المادة الماصة المحضرة (HKUST-1) باستخدام الطريقة الحجمية ، وكانت السعة القصوى لامتزاز البروبان هي (10.499 mmol/g) عند درجة حرارة 298K و ضغط 7 bar. تم فحص نتائج الامتزاز الأيزوثيرمي لفهم توازن النظام (أي الملائمة مع أحد النماذج المعروفة (Freundlich و Langmuir و Temkin) وظهرت نتائج الامتزاز الأيزوثيرمي انها تتناسب بشكل جيد موديل Freundlich. أظهرت النتائج التي تم الحصول عليها من حسابات حرارة الأمتزاز بواسطة معادلة Clausius- Clapeyron أن حرارة الامتزاز تزداد مع زيادة سعة الامتزاز. يمكن استخدام HKUST-1 المحضر والذي يتميز بمساحة كبيرة وقدرة امتزاز عالية كحل رئيسي لتخزين الغاز البترولي المسال (LPG) في المركبات العراقية.

الكلمات الدالة: الأطر العضوية المعدنية, الغاز البترولي المسال, الغاز الطبيعي الممتز, حرارة الأمتزاز.